SULFURIC ACID SPELEOGENESIS IN GREECE

SPELEOGENEZA ŽVEPLOVE KISLINE V GRČIJI

Georgios LAZARIDIS[1], Vasilios MELFOS[2], Lambrini PAPADOPOULOU[2], Bogdan P. ONAC[3,4], Christos L. STERGIOU[1], Angelos G. MARAVELIS[1], Panagiotis VOUDOURIS[5], Despoina DORA[6], Michalis FITROS[7,8], Haritakis PAPAIOANNOU[9] & Konstantinos VOUVALIDIS[6]

Abstract UDC 551.44:546.226-325(495)

Georgios Lazaridis, Vasilios Melfos, Lambrini Papadopoulou, Bogdan P. Onac, Christos L. Stergiou, Angelos G. Maravelis, Panagiotis Voudouris, Despoina Dora, Michalis Fitros, Haritakis Papaioannou & Konstantinos Vouvalidis: Sulfuric acid speleogenesis in Greece

Manifestations of sulfuric acid speleogenesis (SAS) documented in several caves in the areas of Aghia Paraskevi, Konitsa, W. Peloponnese, Elassona, Lavrion and Kammena Vourla in Greece are examined and discussed in this work. Carbonate and sulfate samples collected from caves in Aghia Paraskevi and western Peloponnese areas were investigated using methods, such as fluid inclusion, scanning electron microscopy, carbon, sulfur and oxygen stable isotopes, X-ray powder diffraction, and chemical analysis. The examined caves are mainly developed at or in the proximity of the local water table and they are related to hydrothermal springs and geothermal fields. In addition to the documentation of SAS in one case study from Aghia Paraskevi, calcite spar with a homogenization temperature peak at 280°C, indicates an early speleogenetic stage that involves meteoric-origin hydrothermal fluids under deep-seated settings. Sulfur isotope composition of sulfates (−4‰) is indicative for pyrite oxidation. The Konitsa caves represent a system developed at multiple altitudes that is related to the evolution of Sarantaporos River. The caves in West Peloponnese are located in two different geotectonic units. However, the caves in both units are active and share common characteristics, such as their development near

Izvleček UDK 551.44:546.226-325(495)

Georgios Lazaridis, Vasilios Melfos, Lambrini Papadopoulou, Bogdan P. Onac, Christos L. Stergiou, Angelos G. Maravelis, Panagiotis Voudouris, Despoina Dora, Michalis Fitros, Haritakis Papaioannou & Konstantinos Vouvalidis: Speleogeneza žveplove kisline v Grčiji

V tem delu so proučeni in obravnavani znaki speleogeneze žveplove kisline, dokumentirani v več jamah na območjih zahodnega Peloponeza, Aghia Paraskevi, Konica, Elasona, Lavrion in Kamena Vourla v Grčiji. Karbonatne in sulfatne vzorce, zbrane v jamah na območjih zahodnega Peloponeza in Aghia Paraskevi, smo raziskali z metodami, kot so študija z vključevanjem tekočin, vrstična elektronska mikroskopija, stabilni izotopi ogljika, žvepla in kisika, rentgenska praškovna difrakcija in kemijska analiza. Proučevane jame so nastale večinoma na gladini lokalne podtalnice ali v njeni bližini ter so povezane s hidrotermalnimi izviri in geotermalnimi polji. Poleg dokumentiranja speleogeneze žveplove kisline v eni študiji primera z območja Aghia Paraskevi kalcitni spar z vrhom temperature homogenizacije pri 280°C kaže na zgodnjo speleogenetsko stopnjo, ki vključuje hidrotermalne meteorne tekočine v globokem okolju. Izotopska sestava žvepla v sulfatih (−4 ‰) kaže na oksidacijo pirita. Jame Konica so sistem, ki se je razvil na več nadmorskih višinah in je povezan z razvojem reke Sarantaporos. Jame na zahodnem Peloponezu so v dveh geotektonskih enotah. Vendar so jame v obeh enotah aktivne in imajo skupne značilnosti, na primer vse nastale blizu morske gladine,

[1] Department of Geology, Faculty of Geology, Aristotle University, Thessaloniki, GR-54124, Greece, geolaz@geo.auth.gr

[2] Department of Mineralogy, Faculty of Geology, Petrology and Economic Geology, Aristotle University, Thessaloniki, GR-54124, Greece

[3] School of Geosciences, University of South Florida, 4202 E. Fowler Ave., Tampa, FL 33620, USA

[4] Emil G. Racoviţă Institute, Babeș-Bolyai University, Clinicilor 5, 400006, Cluj-Napoca, Romania

[5] Department of Mineralogy and Petrology, Faculty of Geology & Geoenvironment, National and Kapodistrian University of Athens, Greece

[6] Department of Physical and Environmental Geography, Faculty of Geology, Aristotle University, Thessaloniki, School of Geology

[7] Hellenic Survey of Geology and Mineral Exploration (HSGME), Olympic Village, Acharnae - Athens, Greece

[8] Mineralogical Museum of Lavrion, Attica, Greece

[9] Vikos-Aoos UNESCO Geopark, Greece

GEORGIOS LAZARIDIS, VASILIOS MELFOS, LAMBRINI PAPADOPOULOU, BOGDAN P. ONAC, CHRISTOS L. STERGIOU, ANGELOS G. MARAVELIS, PANAGIOTIS VOUDOURIS, DESPOINA DORA, MICHALIS FITROS, HARITAKIS PAPAIOANNOU & KONSTANTINOS VOUVALIDIS:

sea level, morphology and fracture-guided pattern, and the presence of gypsum with $\delta^{34}S$ values (average –26‰) that are plausibly related to hydrocarbons and bacterial activity. Morphological and geochemical aspects of the caves in these two regions suggest long-lasting, multiphase speleogenetic systems.
Keywords: sulfuric acid speleogenesis, Greece, hydrothermal karst, hypogene caves, cave mineralogy.

imajo podobno morfologijo in prelomni vzorec, poleg tega je v vseh sadra z vrednostmi $\delta^{34}S$ (povprečno –26 ‰), ki so verjetno povezane z ogljikovodiki in aktivnostjo bakterij. Morfološki in geokemijski vidiki jam v teh dveh regijah kažejo na dolgotrajne, speleogenetske sisteme, ki so se razvijali v več fazah.
Ključne besede: speleogeneza žveplene kisline, Grčija, hidrotermalni kras, hipogene jame, jamska mineralogija.

1. INTRODUCTION

Sulfuric acid speleogenesis (SAS) denotes caves formed in carbonate rocks dissolved by sulfuric acid. It is mainly attributed to the type of *"hypogene karstification in unconfined/confined aquifers, partly incised by the erosional network, or side-open to the sea"* (Klimchouk, 2017). This category includes the subtype of *"sulfuric acid speleogenesis, where deep H_2S bearing fluids rise to an unconfined carbonate aquifer and the water table"* (Klimchouk, 2017). However, there are also a few examples of sulfuric acid speleogenesis that are explained by epigene processes (D'Angeli et al., 2019; Webb, 2021; De Waele et al., 2024). Active speleogenesis is quite common among SAS caves, since they are formed at the water table, where the oxidation of hydrogen sulfide is favored. In a thorough review of SAS caves of the world the following definition is suggested *"sulfuric acid speleogenetic caves form through the oxidation of sulfides beneath the land surface, primarily resulting from the interaction between sulfuric acid-rich water and the host rock (mainly carbonates), leading to void creation"* (De Waele et al., 2024). Compared to ordinary caves formed in carbonates by carbonic acid, SAS caves usually contain "exotic" minerals (Polyak and Provencio, 2001; Onac et al., 2009) and gypsum (e.g. Hill, 1995; Swezey et al., 2002). Only a small percentage of caves in carbonates are formed by SAS. In Italy, the country with the most SAS occurrences there is a cave system per ~13.000 km^2 (D'Angeli et al., 2019).

Another interesting aspect of these caves is their relation to hydrocarbon reservoirs that provide hydrogen sulfide, and ore deposits that are formed in phreatic reductive setting (Hill, 1995). Other processes such as microbial or thermochemical sulfate reduction (MSR and TSR, respectively) provide hydrogen sulfide to SAS; mantle degassing in volcanic areas, volcanic activity, and sulfide oxidation may be responsible for hydrogen sulfide enrichment of waters (e.g., Auler and Smart, 2003, De Waele et al., 2024).

In Greece, the best-known SAS cave system is Aghia Paraskevi (Lazaridis et al., 2011), which is the cave type locality of orpiment (Onac and Forti, 2011). Kounoupeli and Anigridon Nimfon caves of western Peloponessus have been described in the exploration report of Merdenisianos (1994). Konitsa and Kammena Vourla caves included in this paper are newly described. Furthermore, there are a few more cases that have been presumed as SAS caves (e.g., Lazaridis, 2017 and references therein). In this paper, morphological studies of these caves along with mineralogical and geochemical analysis provide further evidence on their speleogenetic setting.

2. GEOLOGICAL SETTING

Greece is geologically subdivided into several geotectonic, encompassing external zones (pre-Apulian, Ionian, Gavrovo, Pindos and Parnassos zones) and internal Hellenides zones (Pelagonian, sub-Pelagonian, Attic-Cycladic, Axios, Circum-Rhodope, Serbomacedonian and Rhodope). The investigated SAS cave systems are situated as follow: Kounoupeli, Anigridon Nimfon, and Konitsa (Western Peloponessus) are in the external Hellenides, whereas the Aghia Paraskevi, Kammena Vourla, Peristeri, Psoroneria, Lavrion and Melissotripa are part of the internal Hellenides (Figure 1).

External Hellenides record the shift in geotectonic regime, from an initial extensional (Triassic - early to middle Eocene) to a following compressional (since middle Eocene) setting (Karakitsios, 1995; Zoumpouli et al., 2022). During the extensional phase, external Hellenides experienced crustal stretching and fault-related subsidence that resulted in extensive carbonate sedimentation in a rift-type setting (e.g., Zelilidis et al., 2015; Bourli et al., 2019a, b). The following compressional phase is related to the evolving Pindos Orogen and records siliciclastic sedimentation in a foreland basin system (Botziolis et al.,
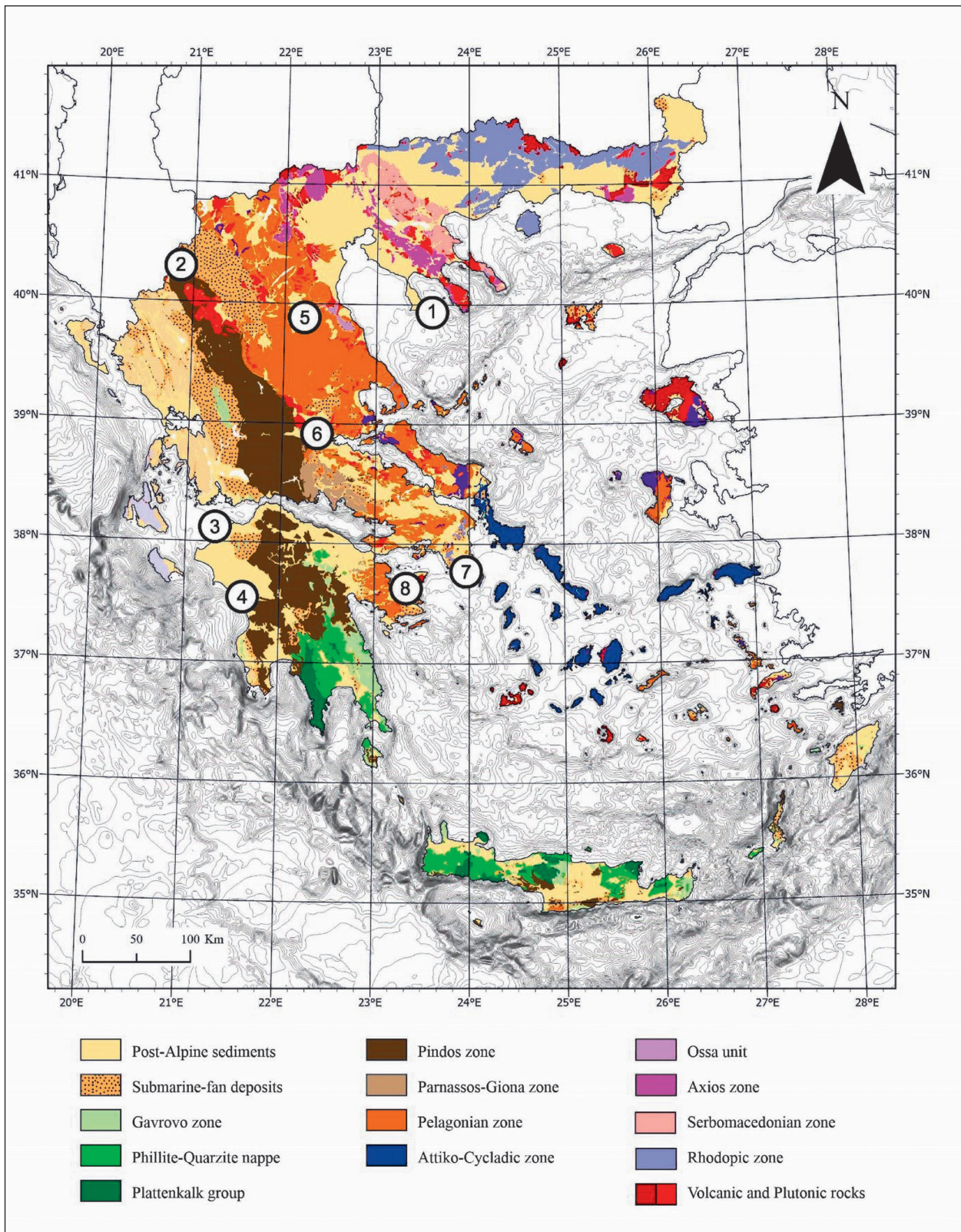
Figure 1: Geotectonic zones of Greece and the distribution of both verified and presumed caves formed by sulfuric acid speleogenesis. 1. Aghia Paraskevi; 2. Konitsa; 3. Kounoupeli; 4. Anygridon Nymfon; 5. Melissotripa; 6. Kammena Vourla and Psoroneria; 7. Lavrion; 8. Peristeri.

2021, 2023). The rock masses of the internal Hellenides include Mesozoic, Paleozoic and older metamorphic rocks that were mainly deformed by the Alpine orogeny and associated tectonics during the Jurassic-Cretaceous. The boundary between internal and external Hellenides is tectonic, with internal Hellenides being overthrusted over the external Hellenides. Geochemical data from the Palaeozoic basement rocks point at a subduction-zone setting, suggesting an active continental margin setting (Pe-Piper et al. 1993; Anders et al. 2005).

3. ANALYTICAL METHODS

Microthermometric data were obtained using a LINKAM THM-600/TMS 90 heating-freezing stage coupled to a Leitz SM-LUX-POL microscope, housed at the Department of Mineralogy, Petrology, Economic Geology of the Aristotle University of Thessaloniki (AUTh). Calibration of the stage was achieved using organic standards with known melting points (chloroform −63.5˚C, naphthalene 80.35˚C, Merck 135 135˚C, saccharine 228˚C, Merck 247 247˚C), and ice (H_2O). The precision of the heating and freezing measurements was ±1°C and ±0.2˚C, respectively. Fluid inclusion shapes and sizes, spatial relationships among inclusions and minerals, and phases within inclusions were observed. The BULK computer package (Bakker 2003) was used to process the fluid inclusion data for calculating salinities and densities.

Mineral inspection and chemical analyses were carried out in the Scanning Electron Microscopy Laboratory, using a JEOL JSM840A Scanning Electron Microscope (SEM) equipped with an Energy Dispersive Spectrometer (EDS) with 20 kV accelerating voltage and 0.4 mA probe current. For SEM observations, the samples were coated with carbon, to an average thickness of 200 Å, using a vacuum evaporator JEOL-4X.

Major element composition was determined by X-Ray Fluorescence (XRF) at the Laboratories of Mineralogy and Petrology of Hellenic Survey of Geology and Mineral Exploration (H.S.G.M.E.), using a S4 Pioneer Bruker AXS (for SiO_2, TiO_2, Al_2O_3, MnO, MgO, CaO, Na_2O, K_2O, P_2O_5, Fe_2O_3 and SO_3).

Calcite samples were analyzed for oxygen and carbon isotope ratios in CO_2 expelled after reacting the carbonate powder for 24 hours with H_3PO_4 at 25˚C. The analyses were performed on a Thermo Delta V isotope ratio mass spectrometer at the Stable Isotope Laboratory, School of Geosciences, University of South Florida (USA). The results are expressed in delta (δ) notation using the following formula: $\delta = (R_{sample}/R_{std} - 1)\cdot1000$, reported in ‰, where R_{sample} is the ratio of $^{13}C/^{12}C$ or $^{18}O/^{16}O$ of carbonates and R_{std} are the same ratios of the international reference standard Vienna PDB (VPDB). Sample δ-value was normalized to the VPDB scale using two reference materials (NBS-18 and NBS-19). Duplicate measurements of the reference materials show that the reproducibility for $\delta^{13}C$ and for $\delta^{18}O$ values is better than ± 0.08‰ and ± 0.06‰ (1σ), respectively.

The sulfur ($\delta^{34}S$) isotope value of sulfate samples was determined following the protocols outlined by Grassineau et al. (2001) and Onac et al. (2011). The analyses were conducted in the Stable Isotope Lab at the School of Geosciences (University of South Florida, USA) using an Elemental Analyzer Costech ECS 4100 and a Temperature Conversion Elemental Analyzer, coupled to a Thermo Fisher Delta V IRMS. The results were normalized to Cañon Diablo Troilite (CDT) based on the $\delta^{34}S$ values of the IAEA standards S-2 and S-3. The reproducibility between replicate standards in each run was better than ±0.1 ‰ (1σ).

4. SULFURIC ACID CAVES OF GREECE

4.1 THE AGHIA PARASKEVI CAVE SYSTEM
Explorations in the Aghia Paraskevi area have uncovered a total of eight small caves, each with its unique characteristics. The first comprehensive study focused on one of these caves, where active sulfuric acid speleogenesis was observed by Sotiriadis in 1969 (Figure 2F), who documented the thermal spring and water chemistry in this cave. Subsequently, Sotiriadis et al. (1982) described another small cave in the area, examining it from the perspective of epigene speleogenesis.

Lazaridis et al. (2011), expanded the speleological evidence in the area, referencing six additional caves
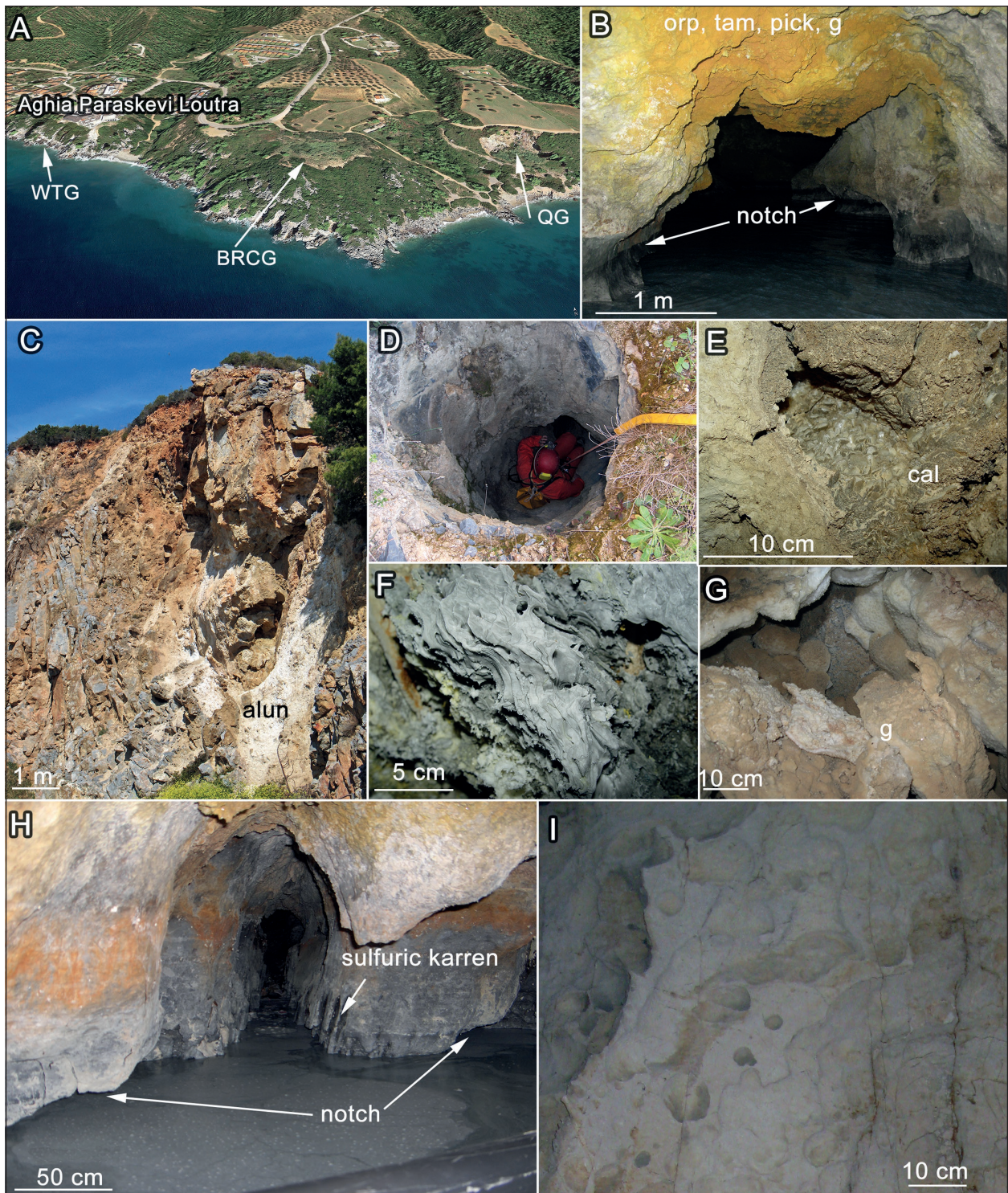
Figure 2: SAS manifestations in Aghia Paraskevi caves. Aerial view of the Aghia Paraskevi area with the locations of the water table (WTG), breakdown (BRCG), and the quarry (QG) group caves. B. Passage in WTG1 Cave with the paragenesis of orpiment (orp), tamarugite (tam), pickeringite (pick), and gypsum (g) on the highest parts and a notch at the water level fluctuation zone. C. View of the QG1 Cave with alunite (alun). D. Entrance of the feeder-like QG2 Cave. E. Phreatic hydrothermal calcite (cal) in QG2 cave. F. Sulfuric acid corrosion on the limestone of Aghia Paraskevi caves. G. Gypsum crust (g) in the deepest part of QG3 Cave. H. Typical passage produced by condensation corrosion in WTG1 Cave, related to notches at the water table and sulfuric karren and the zone of water fluctuation. I. Replacement pockets on the limestone ceiling of QG3 Cave.

GEORGIOS LAZARIDIS, VASILIOS MELFOS, LAMBRINI PAPADOPOULOU, BOGDAN P. ONAC, CHRISTOS L. STERGIOU, ANGELOS G. MARAVELIS, PANAGIOTIS VOUDOURIS, DESPOINA DORA, MICHALIS FITROS, HARITAKIS PAPAIOANNOU & KONSTANTINOS VOUVALIDIS:

and detailing a rare mineral paragenesis that includes orpiment As_2S_3, tamarugite $NaAl(SO_4)_2 \cdot 6H_2O$, pickeringite $MgAl_2(SO_4)_4 \cdot 22H_2O$, and gypsum $CaSO_4 \cdot 2H_2O$. Notably, all the caves in Aghia Paraskevi are a result of hypogene processes and can be categorized into three distinct groups based on their characteristics (Figure 2A).

The first group, designated as the Water Table Group (WTG), comprises three caves situated near the water table along the steep seacoast, featuring thermal water. WTG1 (Figure 2B and 2H), the principal cave housing a thermal spring, spans approximately 15 m in length and 10 m in width, oriented along the N-S and E-W directions, respectively. An unexplored area is situated in its northeast part, mostly covered by a thermal water lake. The cave's ground plan has a ramifying maze pattern, with fracture-guided dissolution forming pillar-like structures in cupola-shaped chambers (Lazaridis et al., 2011, Figure 2A). Notches are visible in various locations, and cm-size wide vertical karren of sulfuric acid origin can be observed in the water fluctuation zone (Figure 2H).

Located about 10 m above the steep seacoast and southeast of WTG1, the vertical entrance to WTG2 cave primarily features an elongated chamber ~15 m long, developed along NNE-oriented fractures. In 2006, thermal water was confined to two small lakes within the cave. To facilitate the operation of the hydrotherapy facility located within the cave, an artificial water recycling system was implemented, directing water from WTG1 to WTG2. Over time, this system caused the water level to rise, eventually covering the entire cave floor.

WTG3 (Figure 2G) is the smallest cave in this group and is located southeast of the other two. It contains small occurrences of the aforementioned sulfate paragenesis. Additionally, several small cavities and vertically developed half-tubes can be found in the proximity of the caves of this group, with sea sand observed at about 10 m above present sea level (mapsl).

The Breakdown Cave Group (BRCG) encompasses two caves positioned at a higher elevation of approximately 40-45 mapsl compared to the others. Both caves are accessible through vertically developed openings: one results from a collapsed sinkhole, while the other is a small cave partially filled with clastic sediments and speleothems. Notably, the latter cave was described by Sotiriadis et al. (1982).

The final group, known as the Quarry Group (QG), comprises three caves discovered during commercial quarry operations. QG1 (Figure 2C) is a sediment-filled cavity primarily containing clastic sediments, and an alunite $KAl_3(SO_4)_2(OH)_6$ layer has been identified in this cave. QG2 is a shaft that spiral downward, featuring a circular cross-section (Figure 2D). Its deepest part is obstructed by rocks. Within the cave passage, fine-grained clastic sediments can be found, with sections lined with phreatic calcite crystals (Figure 2E), a few centimeters in length. These crystals are also present just above the cave entrance. QG3 is a pothole that hosts water ponds at its deepest part. The uppermost part, near the artificial entrance, exhibits chains of cupolas. Gypsum crusts (Figure 2G) occur on the lower parts of the passage, along with replacement pockets (Figure 2I) and cupolas on the ceiling. In specific locations within the clastic sediments, we have observed rounded clasts approximately 10 cm in diameter. These clasts are composed of gypsum and are believed to have replaced the original limestone.

4.2 WESTERN PELOPONNESE: KOUNOUPELI AND ANIGRIDON NIMFON CAVES

In the western region of the Peloponnese, two caves characterized by active thermal springs and SAS are noteworthy. The Anigridon Nymfon Cave is situated within the limestone formations of the Gavrovo Zone (Figure 1). This relatively small cave, measuring approximately 70 m in length and covering an area of around 340 m², is documented in a study by Merdenisianos (1994). The cave is primarily a single passage extending in a NNW-SSE direction. A thermal water lake, rich in hydrogen sulfide, extends to the entire cave area. Towards its deepest point, the passage's size gradually decrease to the point of becoming impassable. An analysis of gas seepage in NW Peloponnese by Etiope et al. (2006) revealed that the thermal springs are notably abundant in thermogenic methane originating from deep Mesozoic limestone reservoirs, and the hydrogen sulfide is most probably of TSR origin; in which sulfur compounds, particularly sulfate minerals, undergo reduction at high temperatures.

The Kounoupeli Cave (Figure 3) is situated in the Late Triassic to Eocene carbonates, lying above the Triassic evaporites and beneath the Oligocene flysch of the Ionian Zone (Figure 1). These rock formations appear to give rise to mega-synclines and anticlines. Located at sea level and just a few meters from the coastline, this active sulfuric acid cave is ~50 m in length. It consists of a fracture-guided corridor with segments oriented along the N–S and E–W directions (Figure 3A). Gypsum crust partially covers side walls (Figs. 3B and 3C). Morphologically, the passage features a triangular cross-section with a flat floor and a central channel (Figs. 3D; 3E and 3F). Moreover, water-table notches can be observed on the cave walls (Figs. 3D and 3F).
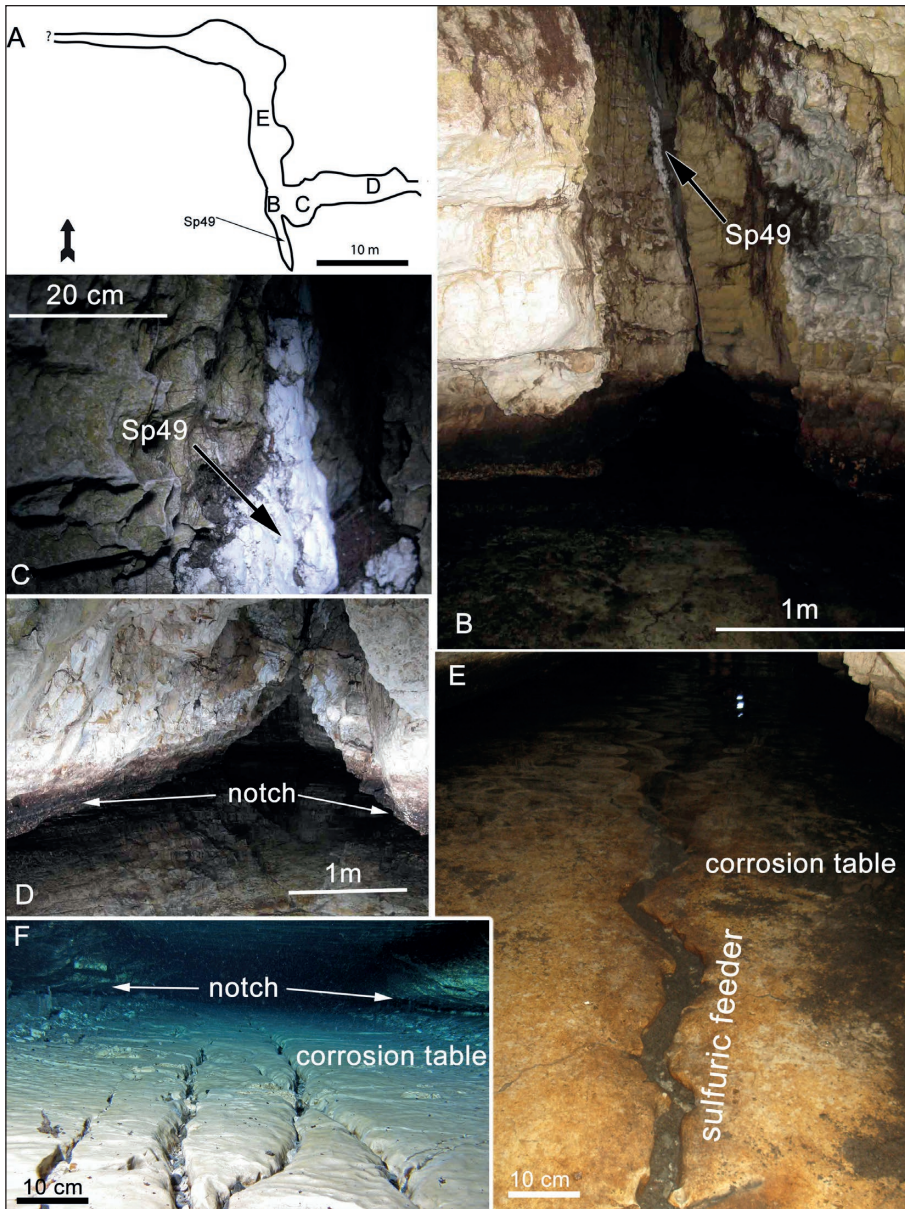
Figure 3: SAS manifestations in the Kounoupeli Cave. A. Plan of Kounoupeli Cave (letters indicate position of photos). B. Gypsum deposits identified as light-colored patches on the wall. C. Close up view of gypsum sample Sp49. D. View of the N-S gallery. E. Corrosion table and sulfuric feeder that form the floor of the cave. F. Underwater photo (courtesy of Vasilis Athanassopoulos) of the flat floor that forms a corrosion table.

4.3 KONITSA

Numerous caves related to SAS have been explored in Konitsa region, with the most striking ones being associated with the evolution of the Sarantaporos River. These caves have been developed within the limestone formations on both sides of the riverbanks in the localities of Pixaria Loutra and Skordyli Bridge (Figure 1). In the latter location, a series of small caves are distributed at different elevations, representing successive stages of speleogenesis that extending up to several tens of meters above water level. Presently, these caves are mostly inactive and undergoing recession due to erosion. However, Skordyli Cave is the largest in the area and is still active.

It has a spacious main gallery (Figure 4A) that display multiple notches (Figure 4B) and dome-shaped chambers (Figs. 4C and 4D). A flat corroded stream bed with gypsum deposits featuring a thermal spring abundant in hydrogen sulfide that support the formation of whitish stream biofilms (Figure 4E). Along with multiple notches, clastic sediment banks can be seen in some cave areas (Figure 4F).

Within the large cave, eroded clastic sediments and notches have formed concurrently with a drop in the local water level. Hydrogen sulfide concentrations up to 2 ppm has been detected in the deeper sections of the cave.

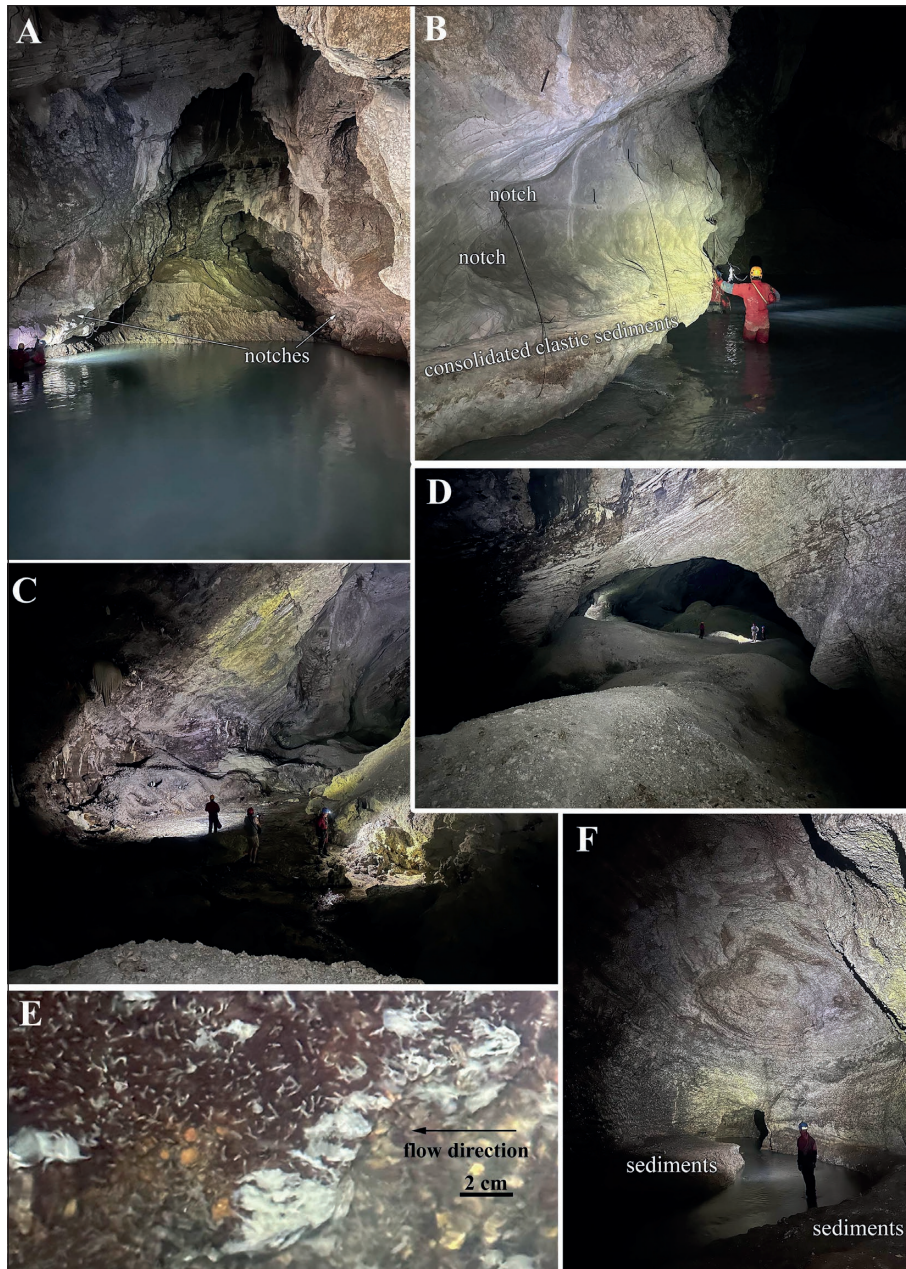Pixarias Cave is located in close proximity to Pixaria

Figure 4: SAS manifestations in the Skordyli Cave. A. Entrance area of the Skordyli Cave. Note the sulfur-rich water that floods the entire chamber. Notches can be seen in both sides, along with eroded consolidated clastic sediments. B. Detail of the close-spaced notches and the consolidated sediments. C. View of the deepest part of the cave. D. Part of the main corridor at its widest point; the sulfuric stream flows at lower altitude at the right side of the passage. E. Whitish filamentous microbial structure in the sulfuric stream. F. A narrow part of the main passage where the stream flows in the middle of eroded clastic sediments.

thermo-mineral spring and has a maze pattern (Figure 5A). The cave passages follow structural discontinuities along joints and are relatively uniform in size, extending in various directions that interconnect at multiple points. In cross-section, they show multiple distinctive characteristics of SAS (Figure 5B). These passages exhibit bilateral symmetry, with the vertical axis aligning with the joint that guides the dissolution process by providing hydrogen sulfide.

The lower section of the passage narrows into a vertical crevice, where the width diminishes with depth. At the end of this central channel, an approximately hori-zontal floor forms. This floor is marked by numerous grooves, a few centimeters in width, transversely oriented concerning the passage. These grooves connect with smaller channels, creating a small-scale hydrographic network that correspond to sulfuric acid-derived karren.

Above the floor, notches can be observed in both side-walls (Fig 5B). The upper part of the passage is notably wider than the portion below the floor level and may contain gypsum deposits in several locations (Figure 5C).

The cave has a mostly flat floor with a subtle inclination of approximately 1° towards the Sarantaporos River (Figure 5D). It is worth noting that the limestone beds

dip 20° towards SW, so the flat cave floor is a result of dissolution processes rather than structural control.

In the Pixaria Cave, several elliptical pond-like areas exist, all with a coarse surface on the floor. The central portion of these areas is influenced by sulfuric feeders.

The surface of the ponds exhibits smaller depressions and sulfuric acid-formed karren. We examined two specific cases, each displaying variations in morphology.

The first sulfuric pond (Figure 6A) is characterized steep walls, suggesting that it is a result of simultaneous
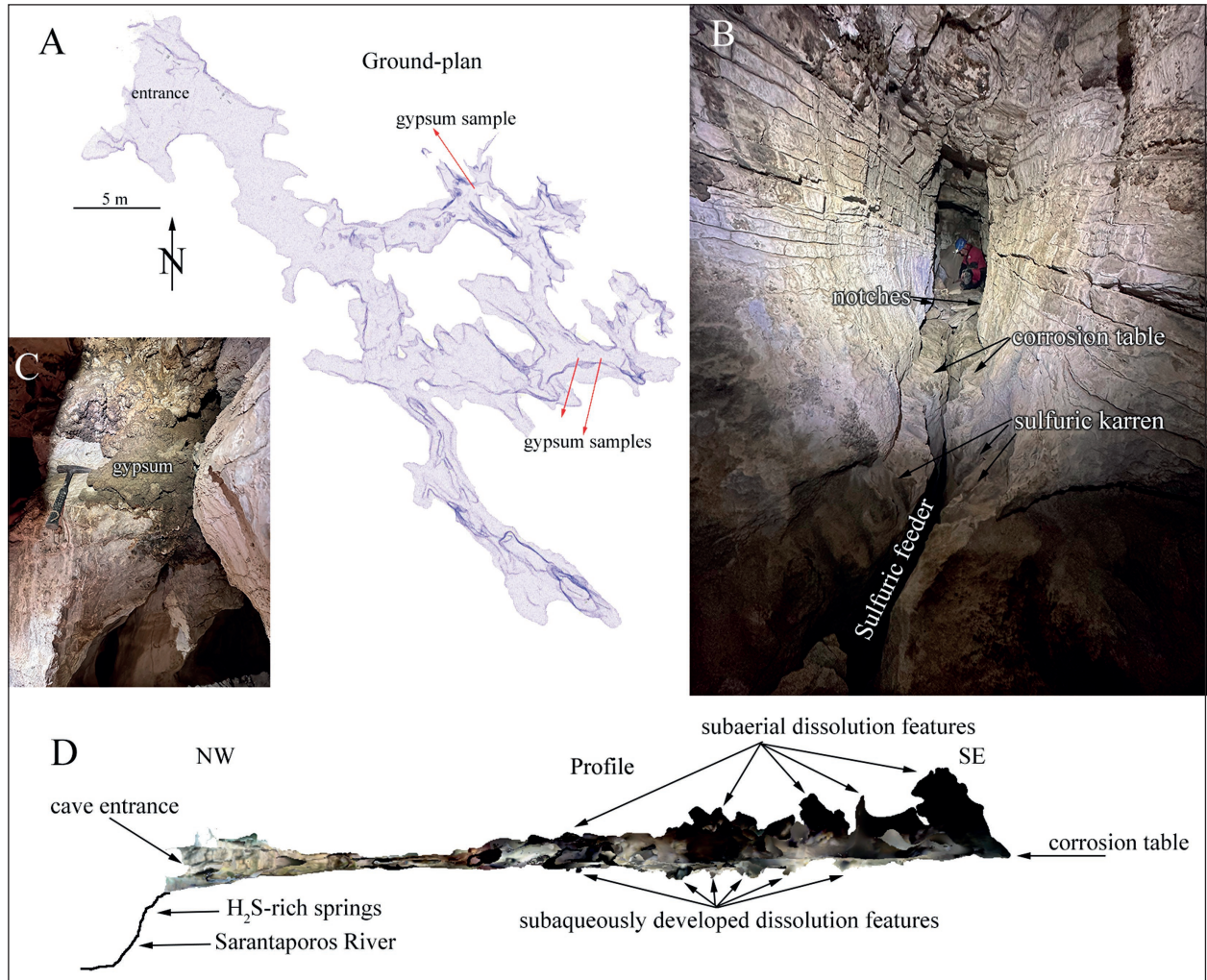

Figure 5: SAS manifestations in the Pixarias Cave. A. Ground-plan. B. Typical passage morphology with a medial discharge feeder, a flat floor that corresponds to the corrosion table overprinted by sulfuric karren and a pair of notches formed just above that table. C. Gypsum deposits on the cave walls. D. NW-SE profile on which limited dissolution below the corrosion table can be seen and the level of springs and Sarantaporos River.

Figure 6: Origin of sulfuric karren in Pixaria Cave by: A. Simultaneous dissolution from various feeders. B. Water level drop.

dissolution from multiple feeders. Its surface is characterized by sulfuric karren with concentric arrangement. This form reflects the interplay of sulfuric processes in shaping its morphology.

The other pond (Figure 6B) is delimited by steep walls and has a stair-like floor surface dominated by small-sized few centimeters wide depressions. It is suggested to have formed due to a drop in the water level, leading to the concentration of sulfuric water in the lowest central part of the passage. This process results in a distinct morphology, marking a different origin for this particular pond.

4.4 KAMENA VOURLA CAVE

A cave-spring is situated along the escarpment of the active Kamena Vourla fault zone, as documented in studies by Ganas et al. (1997) and Cundy et al. (2010). The cave passage is flooded (Figure 7), and the presence of hydrogen sulfide is detectable in the cave atmosphere. Exploration of this cave has been limited, reaching only the first chamber, located approximately 10 m from the entrance.

Figure 7: Entrance passage of Kammena Vourla spring-cave.

4.5 THE PERISTERI CAVE IN METHANA PENINSULA

This cave is located in Methana Peninsula in the eastern part of Peloponnese and comprises the westernmost part of the south Aegean volcanic arc (Figure 1:8). Its entrance is formed due to ceiling collapse (Petrocheilou, 1974). Although it has been referred as related to SAS (Lazaridis, 2017), further investigation is needed to verify the contribution of sulfuric acid speleogenesis in the formation of the cave.

4.6 PSORONERIA CAVES

Some small inactive caves (Figure 8) that occur next to the thermal sulfuric water spring of Psoroneria, in the vicinity of Kamena Vourla. They lack typical morpho-

Figure 8: Morphology of Psoroneria caves with large voids and wide entrances.

logical indicators and gypsum deposits and they need further research to interpret their origin.

4.7 LAVRION CAVES

Recently, some natural dissolution caves cut by mining galleries in Lavrion mines (see 7 in Figure 1 for location) have been identified and are under investigations from a speleogenetic and ore deposit perspective.

One of these cavities discovered in the Paleokamariza #18 Mine, displays morphologies with cupola-related features, gypsum and dolomite with quartz, celestine, opal-AN, cinnabar, gorceixite $BaAl_3[(PO_3(O,OH)]_2(OH)_6$, coronadite $Pb(Mn^{4+}_6Mn^{3+}_2)O_{16}$, iron hydro/oxides, as well as a number of supergene uranium minerals: andersonite $Na_2Ca(UO_2)(CO_3)_3 \cdot 6H_2O$, bayleyite $Mg_2(UO_2)(CO_3)_3 \cdot 18H_2O$, boltwoodite $(K_{0.56},Na_{0.42})(UO_2)(SiO_3OH) \cdot 1.5H_2O$, chadwickite $(UO_2)H(AsO_3)$, lanthinite (non-uranium) $La_2(CO_3)_3 \cdot 8H_2O$, nováčekite $Mg(UO_2)_2(AsO_4)_2 \cdot 10H_2O$, sklodowskite $Mg(UO_2)_2(SiO_3OH)_2 \cdot 6H_2O$, uranospinite $Ca(UO_2)_2(AsO_4)_2 \cdot 10H_2O$, uranophane $Ca(UO_2)_2[SiO_3OH]_2 \cdot 5H_2O$, uraninite UO_2 (Rieck et al., 2018; Ottens and Voudouris, 2018; Vourlakos and Fitros, 2019).

The deposition of gypsum and all associated minerals could be related to SAS of either hypogene, but most probably epigene processes.
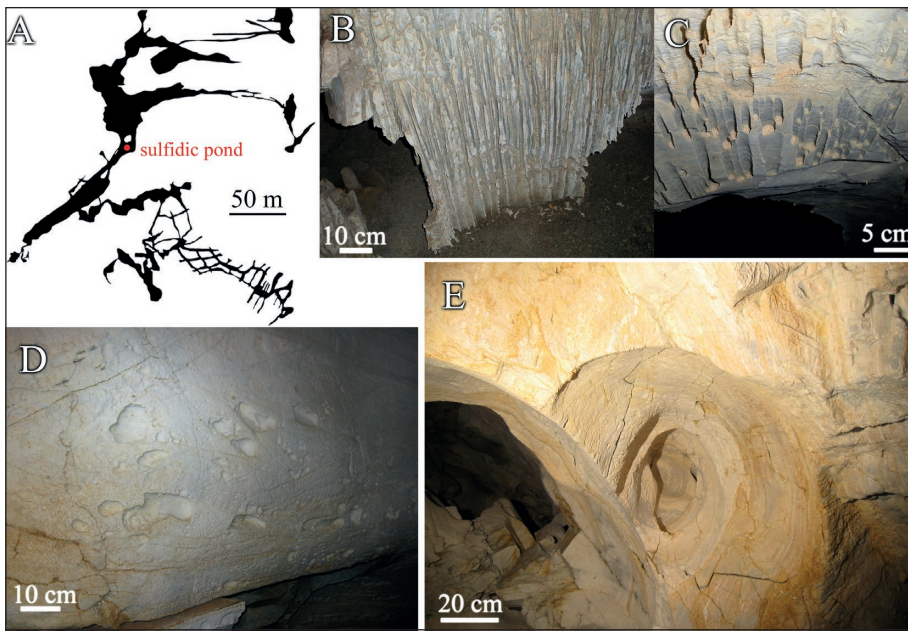
Figure 9: SAS manifestations in Melissotripa Cave. A. Ground-plan pattern of the cave. B–C. Sulfuric karren formed by dripping-seeping water. D. Replacements pockets on the limestone walls. E. Intersected cupolas.

4.8 THE MELISSOTRIPA CAVE IN ELASSONA

Melissotripa encompasses a total passage length of approximately 2.1 km, with large galleries forming a maze area (Figure 9A). It has developed within a carbonate unit right beneath the schists-gneisses of the Pelagonian massif (Figure 1). The largest chambers within the cave have undergone significant modifications due to extensive breakdown, while the section formed beneath the caprock primarily exhibits a two-dimensional maze-like pattern.

This cave has been proposed as a hypogene cave with SAS in confined conditions, attributed to the presence of phreatic cupolas, gypsum in blister speleothems, and the detection of hydrogen sulfide in a small water pond believed to be connected to the local aquifer (Vaxevanopoulos, 2006). However, we interpret the presence of cupola morphology in the cave as the result of condensation corrosion. Lazaridis (2017) documented sulfuric karren (Figs. 9B and 9C) and replacement pockets (Figure 9D) within the cave, including it among Greece's hypogene caves. The cave's two-dimensional

maze section and the schists-gneisses overlaying the carbonates acting as a caprock, suggest a hydrological setting conducive to hosting hypogene processes.

The cave extends to an elevation of 251.7 mapsl, whereas the average water table elevation was approximately 256 mapsl for the period 1988-1992 (Manakos, 1999; Vasileiou & Koumantakis, 2013). This indicates that the small lakes within the cave are linked to the local karst aquifer, primarily developed in the carbonate formations of Krania, with no significant sulfur content. In fact, higher concentrations of sulfate ions (SO_4^{2-}) were detected in surface water samples when compared to groundwater samples (Manakos et al., 2018). The karst water in the region is of Mg-HCO_3^- type and discharges at a contact spring along a fault that also intersects the cave entrance.

Given the absence of sulfur in the aquifer and considering well-documented instances of epigene-based SAS processes elsewhere (e.g., Angeli et al., 2019; Webb, 2021), the origin of SAS in Melissotripa is subject of further investigation.

5. MINERALOGICAL AND GEOCHEMICAL RESULTS

Mineralogy and geochemistry have been studied in two distinct areas with SAS. The first area of Aghia Paraskevi belongs to the Internal Hellinides and the second one in western Peloponessus belongs to the External Hellinides. They are both located in coastal areas and therefore they

have been considered as comparable examples. Through their analysis it is attempted to interpret their evolution and to identify differences depending on the geological setting.

Fluid inclusions data were obtained from a calcite sampled from the QG2 Cave. The results are presented in
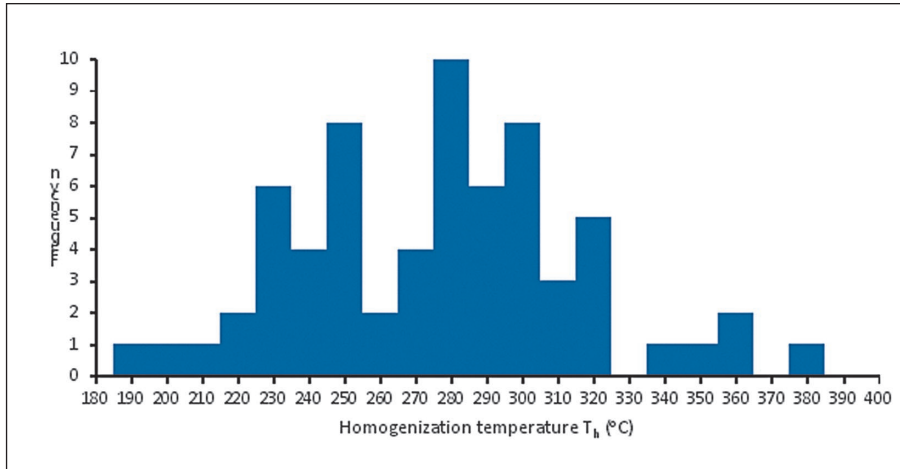
GEORGIOS LAZARIDIS, VASILIOS MELFOS, LAMBRINI PAPADOPOULOU, BOGDAN P. ONAC, CHRISTOS L. STERGIOU, ANGELOS G. MARAVELIS, PANAGIOTIS VOUDOURIS, DESPOINA DORA, MICHALIS FITROS, HARITAKIS PAPAIOANNOU & KONSTANTINOS VOUVALIDIS:

Figure 10: Histogram of homogenisation temperatures measured in the fluid inclusions of Sp9/PAR(B) sample from QG2 Cave in Aghia Paraskevi.

Figure 10. At room temperature, only two phase liquid-vapor inclusions were identified. Inclusions that were analyzed, ranged in diameter between 5 and 70 μm and display homogenization into the liquid state. Vapor to liquid ratio is 1–20 vol % μm with some exceptions that exceed 50%. The variability in homogenization temperature data may be due to real variability in the fluid inclusion assemblages or to post-entrapment processes such as thermal re-equilibration or undetectable necking-down (Goldstein, 2003). Homogenization temperature ranges from 183 to 380 °C with a peak at ~280 °C (n=67). The initial melting temperature (Tfm) is approximately −21.2 °C, indicating that the main components of the fluid are H_2O and NaCl. The salinity ranges from 1.91 to 3.39 wt% NaCl.

Isotopic composition of calcite and gypsum samples, and chemical analysis from the caves of Aghia Paraskevi are given in Supplementary Information (Tables 1 and 2). The calcite display traces of Fe, Mn, K, Na, S, P, Ti, As, Rb, and Sr. The gypsum is characterized by a high arsenic content (1754 ppm).

Investigations were conducted on gypsum samples Sp47 and Sp 49-51 from Anigridon Nymphon and Kounoupeli caves in the Peloponnese. SEM was used to examine samples Sp49, Sp50, and Sp51. The Sp49 sample was found to consist of small gypsum crystals, ranging
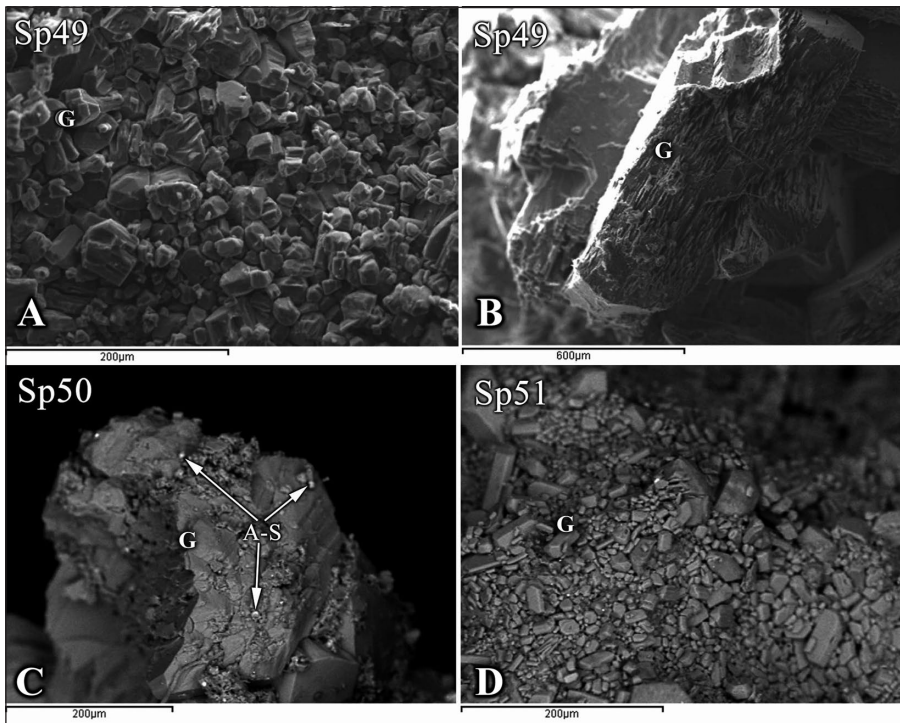

Figure 11: Scanning Electron Microscope (SEM) images of gypsum samples from the cave at Kounoupeli. A. and B. The images showcase the size and shape of gypsum crystals (G); C. some alumino-silicate minerals (indicated as A-S) in the Sp50 sample; D. gypsum of sample Sp51.

in size from 5 to 50 μm (Figure 11). Both Sp50 and Sp51 contain gypsum along with aluminosilicate minerals (as shown in Figure 11), but Sp50 is particularly iron-rich.

Semiquantitative SEM-EDS chemical analysis of the Kounoupeli aluminosilicate minerals found in sample Sp51 and the XRF chemical analysis of gypsum are given in Supplementary Information (Tables 3 and 4). Isotopic composition of gypsum samples from the caves of W. Peloponnese are included in Supplementary Information (Table 5).

6. DISCUSSION

Among the cave examples discussed here, Aghia Paraskevi and Konitsa caves in Northern Greece, Kounoupeli and Anigridon Nimfon caves in western Peloponnese, stand out as regions in Greece with the best-documented instances of hypogene sulfuric acid speleogenesis. In other areas, either SAS has not been fully confirmed yet (as in the cases of Peristeri and Psoroneria), or its role in the cave formation remains unclear, as is the case with Melissotripa Cave and the Paleokamariza #18 Mine. Moreover, some caves remain unexplored, including the Kamena Vourla spring-cave.

6.1 STAGE OF CAVE EVOLUTION

The Aghia Paraskevi caves are categorized into three groups based on their stage of development, resulting in distinctive morphologies. It appears that the caves' elevation corresponds to their age, with higher caves being older. The WTG, primarily hosting active SAS caves, exhibits a unique orpiment-bearing paragenesis (Lazaridis et al., 2011).

The Quarry Group caves contain calcite spar with high homogenization temperatures, as well as alunite and gypsum related to SAS development. The high calcite homogenization temperature and the passage morphology indicative of formation in phreatic conditions, suggest a deep-seated speleogenetic setting. The homogenization temperature and salinity of the fluid inclusions in the calcite, compare well with data from basinal, seawater, meteoric, metamorphic, and magmatic hydrothermal ore-forming fluids (Kesler, 2005). A meteoric origin for the fluids is suggested due to their increased homogenization temperature and relatively low salinity. The calcite bearing passages in Aghia Paraskevi caves are formed in depth as indicated by the homogenization temperature and then they have been uplifted. A similar succesion can be found in the Provalata Cave in North Macedonia, which shows an early phase of carbonic acid speleogenesis followed by SAS (Temovski et al., 2013, 2018). Azerou hydrothermal and sulfuric karst in Algeria is another example of these successive speleogenetic events (Audra, 2017).

The positive $\delta^{13}C$ value of the calcite suggests that the isotopic composition of the bedrock rather than soil CO_2 dominate the $\delta^{13}C$ record. This is likely related to a pyrite oxidation process that drives the acidity needed for bedrock dissolution. An additional evidence of pyrite oxidation could be the $\delta^{34}S$ values (−4‰) measured in sulfate crusts from several caves in this area. Furthermore, gypsum crusts in QG3 Cave, associated with SAS at or near the water level, contain a high concentration of arsenic (1754 ppm), commonly found in the thermal waters of the region and in the orpiment paragenesis observed in the water table caves of the area (Lazaridis et al., 2011). Similarly, the hydrothermal calcite that more difficult incorporates arsenic (e.g. Fernandez-Martinez et al., 2006), displays a concentration of 10 ppm.

Likewise Aghia Paraskevi caves, the cave system in Konitsa includes multiple cavities at different elevations. Those at river level are still active, representing another example of SAS with a complex geological history influenced by the uplift rates of the area and the downcutting rate of the Sarantaporos River.

The genesis of caves in W. Peloponnese is closely tied to sea level fluctuations. However, the existence of submerged inactive SAS cave passages in these regions cannot be ruled out, as they have not yet been explored. In fact, the mean sulfur isotopic composition (∼ −26‰; see Table 5 in Supplementary Information) suggests the presence of SAS, with H_2S sourced from low-temperature microbial sulfate reduction. Comparable $\delta^{34}S$ values have been reported from numerous SAS caves worldwide (for a review, see De Waele et al., 2024).

In conclusion, we can distinguish three major stages of evolution for these cave systems:
- Initial hydrothermal speleogenesis: characterized by carbonic acid-driven processes in deep settings, with the possible co-occurrence of SAS at the water table.
- Active SAS caves: associated with the water table.
- Inactive SAS caves: occur due to relative water table drop caused by uplift and denudation, leading to the formation of tiered cave levels and remnants of SAS above the water table. The rise of the water table may have submerged already formed SAS caves.

6.2 CONTROL OF TECTONOSTRATIGRAPHIC SETTING ON THE FORMATION OF SAS SYSTEMS

The density of hypogene SAS caves in Greece is one per ~26.000 km². This high density is only second to Italy, where about 25% of the worldwide known SAS caves have been discovered (D'Angeli et al., 2019). This abundance of SAS systems in Greece could be associated with the regional tectonostratigraphic setting.

The caves in W. Peloponnese (Kounoupeli Cave and Anigridon Nimfon) and Konitsa are situated in western Greece, a region that was under extension throughout the Mesozoic and under compression since Early to Middle Eocene due to modifications in the motion of the Apulian and Pelagonian plates (e.g., De Graciansky et al., 1989; Doutsos et al., 1993). The extensional period displays the ongoing evolution of a rift-type setting, from the pre- to syn-rift stage, and is characterized by the sedimentation of carbonates (Karakitsios, 1995; Bourli et al., 2019a, b). As such, Upper Triassic to Lower Jurassic shallow marine limestones are deposited over Triassic evaporites. The Late Eocene shift in tectonic regime, from extensional to compressional, occurred because of the Pindos Orogen and is accompanied by a shift in sedimentation, from carbonate to siliciclastic. Such deposits are intensively deformed by contractional tectonics during the upbuilding and westward migration of the Pindos fold and thrust belt (Botziolis et al., 2021; 2023).

Within this tectonic framework, a network of deep faults (both normal and reverse) cut across the entire regional stratigraphic succession. These faults serve(d) as potential pathways for the ascent of deep-seated sulfidic fluids through the stratigraphic column, reaching shallow levels and forming the studied caves in western Peloponnesus. As these solutions ascended sulfate reduction led to the formation of hydrogen sulfide, which subsequently oxidized near the surface, triggering the development of sulfuric acid caves. A similar mechanism has been invoked by D'Angeli et al. (2019) to explain the abundance of SAS systems in Italy.

Likewise Italy, Greece shares similar geotectonic evolution since Mesozoic, thus, the source of sulfidic fluids might have been the Triassic evaporates. Another possible scenario that could form SAS systems is the interaction of hydrocarbons with evaporitic rocks in the lithological successions. The External Hellenides in the western Greece, share geological similarities with the External Albanides in the neighboring region of Albania. A study by Klimchouk et al. (2022) in Albania's External Albanides, relate SAS with geothermal reservoirs and hydrocarbons discovered at a depth of 3,000 m. This suggests that the geological conditions supporting hydrocarbons in Albania may extend into western Greece (e.g., Maravelis et al., 2012). The formation of these features is thought to be connected to the geotectonic evolution of the region from the Upper Miocene to Pleistocene. This period witnessed the uplift and erosion of the flysch cover, which in turn triggered artesian water flow through carbonate rocks, concurrently initiating hypogene speleogenesis. Similar consideration has been proposed for the caves of the Guadalupe Mountains that developed when upward moving H_2S originating from the oil fields of the Delaware Basin, oxidized to sulfuric acid close to the water table (Hill, 1995).

6.3 CAVE MORPHOLOGY

Fracture-guided cave morphology: In their entirety, the investigated caves exhibit single fracture-guided passages (e.g., Kounoupeli Cave), ramifying mazes (e.g., WTG1 in Aghia Paraskevi), network mazes (e.g., Pixarias Cave), conduits with sizable chambers affected by breakdown (e.g., Skordyli Cave), and vertically developed feeders (e.g., QG2 in Aghia Paraskevi). These feeders are predominantly linear and tectonically guided.

Sulfuric acid-induced dissolution contributes to speleogenesis in both subaqueous and subaerial conditions near the water table (e.g., De Waele et al., 2016). The latter is more dominant, particularly under specific conditions involving the flow of H_2S-rich waters (Jones et al., 2015). A number of meso- and micro-scale dissolutional features observed in the studied caves are considered SAS morphologies. These include notches, corrosive table, dome-shaped pockets, floor elongated feeders, and sulfuric karren. All these features are susceptible to changes during later phases of cave development.

In the caves of western Peloponnese, particularly in Kounoupeli Cave, where one level of lateral notches is present, the dissolved bedrock volume above the notches is considerably higher than that below the water table. This is indicative of significant subaerial SAS.

From a few cross-sections in Pixarias Cave, we estimate that the notch level is about 10% of the cross-section, the feeder is 20%, and the domes represent 70%. The maximum width of the subaerially dissolved cross-section part is 40% wider than the notch level and more than four times the width of the feeder. This implies that dissolution above the water table is favored. However, in larger passages, like those in Skordyli Cave, where breakdown plays a significant role in its development, the subaerial portion becomes even more extensive.

The extensive morphology of SAS caves includes cupolas and a variety of speleogens that result from the interconnection of several cupolas, such as megascallops, cusps, windows, bridges, and more. While these features are found in most known examples of this cave type, they are polygenetic (e.g., Plan et al., 2012; Dublyansky, 2013; De Waele et al., 2016). Notches, although possibly unre-

lated to cupolas, also exhibit polygenetic characteristics in terms of chemical reactions (sulfuric and carbonic acids can create notches) and erosion *sensu lato* processes (e.g., paragenesis; Farrant and Smart, 2011). However, when formed as pairs of identical notches at the same level, they serve as markers for the water table.

Subaerial and subaqueous sulfuric karren and other small-scale forms such as drip tubes, pendant drip holes, and cups are mentioned in other case studies (Audra et al., 2009; De Waele et al., 2016). Notably, karren is a collective term that includes dissolutional features of various morphologies and sizes. In this work we described both subaqueously and subaerial karren. Subaerial sulfuric karren corresponds to the drip tubes described by Audra et al. (2016), whereas the subaqueously ones can be found in caves such as WTG1 (Figure 2H) and Pixarias (Figure 6), where they form in the zone influenced by water level fluctuations, appearing on lower walls sections and corrosion tables. Another type of sulfuric karren reported in Melissotripa Cave (Lazaridis, 2017), consist of a dense network of channels originating from drip holes, approximately 1 cm in diameter and running downward on inclined surfaces for several decimeters; they indicate a subaerial origin. Given that dripping points are unrelated to pendants or cusps, an additional factor contributing to dense dripping points should be considered and further investigated. A reasonable hypothesis would assume that biofilms would have been existed and were able to supply strong acid drips, referred as snottite (Barton et al., 2007). Although these forms are highly distinctive, they have not been observed in other caves included in this study.

Replacement gypsum pockets are prominent features in SAS caves, that are easily recognizable and morphologically they strictly define this type of speleogenesis.

6.4 GEOMORPHOLOGICAL CONTROL
In the vicinity of and above the water table, the presence of high oxygen levels enables the oxidation of hydrogen sulfide, making SAS caves remarkable indicators of previous water table levels (e.g. Hill, 1995; Audra et al., 2015; De Waele et al., 2016). Greece highlights notable examples of SAS in locations linked to hydrothermal springs. These areas involve the mixing of water with seawater, discharging at or near sea level, or combining with meteoric water and discharging in an incised valley. While inactive SAS caves at higher elevations than their active counterparts have not yet been documented in western Peloponnese, Aghia Paraskevi presents a unique case. It features relict caves displaying distinct SAS mineralogical and morphological characteristics, suggesting a complex evolutionary history involving sea-level changes, climatic variations, and tectonic uplift.

7. CONCLUSIONS

In the systematic investigation of Greek cave systems originating from SAS, several key observations and conclusions emerge. The study highlights the widespread occurrence of SAS systems in Greece, attributed to the dynamic geotectonic settings of the region. The cave systems in Greece are intrinsically linked to an ever-changing interplay of factors, including environmental conditions, geological uplift, and sea-level fluctuations. These dynamic variables influence the positioning of the water table and, consequently, the formation of these caves. The presence of deep faults, hydrothermal activity, volcanism, ore-forming processes, and potentially hydrocarbon reservoirs, make Greece ranking as the second-highest country in terms of SAS distribution per square kilometer.

Based on their geological origin and historical evolution we identified: caves formed by deep-seated carbonic acid and later modified by SAS, active, and inactive SAS caves.

While the morphological characteristics of the dissolutional features within these caves may exhibit polygenetic origins, they also display unique characteristics that are indicative of SAS. These include replacement pockets, particular passage cross sections with dissolution forms below the water table markers, floor ponds, and subaerial sulfuric karren.

Despite the limited data available, the isotopic values of sulfate minerals within the investigated caves can be divided into two distinct groups: In the Aghia Paraskevi caves the $\delta^{34}S$ values suggest pyrite oxidation, whereas the in W. Peloponnese the values indicate microbial sulfate reduction of gypsum hosted in the sedimentary sequence in the presence of hydrocarbons.

The relationship between these caves and the water table makes them excellent markers for tracking past water table levels. Given the constant changes in the water table in the studied cases due to uplifting, down-cutting, and sea-level changes, the formation of sulfuric acid dissolved cave passage at various levels is anticipated to have been occurred rapidly.

In summary, the systematic exploration of SAS-driven cave systems in Greece sheds light on the complex interplay of geological, environmental, and hydrogeological factors shaping these unique underground environ-

ments. The presence of distinct morphological features and mineralogical compositions further highlights the exceptional nature of these cave systems and their utility in understanding geological processes.

ACKNOWLEDGMENTS

REFERENCES

Anders, B., Reischmann, T., Poller, U., Kostopoulos, D., 2005. Age and origin of granitic rocks of the eastern Vardar Zone, Greece: new constraints on the evolution of the Internal Hellenides. Journal of the Geological Society of London, 162: 857–870. https://doi.org/10.1144/0016-764904-077

Audra, P., 2017. Hypogene Caves in North Africa (Morocco, Algeria, Tunisia, Libya, and Egypt). In: Klimchouk, A., Palmer, A. N., De Waele, J., Auler, A. S., Audra, P. (eds) Hypogene Karst Regions and Caves of the World. Cave and Karst Systems of the World, pp. 853-864 Springer, Cham.

Audra, P., Mocochain, L., Bigot, J. Y., Nobécourt, J. C., 2009. Morphological indicators of speleogenesis: hypogenic speleogens. Hypogene speleogenesis and karst hydrogeology of artesian basins. Simferopol: Ukrainian Institute of Speleology and Karstology, Special Paper 1: 23-32.

Audra, P., Gázquez, F., Rull, F., Bigot, J.-Y., Camus, H., 2015. Hypogene Sulfuric Acid Speleogenesis and rare sulfate minerals in Baume Galinière Cave (Alpes-de-Haute-Provence, France). Record of uplift, correlative cover retreat and valley dissection. Geomorphology, 247: 25-34. https://doi.org/10.1016/j.geomorph.2015.03.031

Auler, A. S., Smart, P. L., 2003. The influence of bedrock-derived acidity in the development of surface and underground karst: evidence from the Precambrian carbonates of semi-arid northeastern Brazil. Earth Surface Processes and Landforms: The Journal of the British Geomorphological Research Group, 28(2): 157-168. https://doi.org/10.1002/esp.443

Bekker, R.J., 2003. Package FLUIDS 1. Computer programs for analysis of fluid inclusion data and for modelling bulk fluid properties. Chemical Geology, 194 (1-3), 3-23.https://doi.org/10.1016/S0009-2541(02)00268-1

Barton, H. A., Taylor, N. M., Kreate, M. P., Springer, A. C., Oehrle, S. A., Bertog, J. L. (2007). The impact of host rock geochemistry on bacterial community structure in oligotrophic cave environments. International Journal of Speleology, 36, 93-104.

Botziolis, C., Maravelis, A., Pantopoulos, G., Kostopoulou, S., Catuneanu, O., Zelilidis, A, 2021. Stratigraphic and paleogeographic development of a deep-marine foredeep: Central Pindos foreland basin, western Greece. Marine and Petroleum Geology, 128, 105012. https://doi.org/10.1016/j.marpetgeo.2021.105012

Botziolis, C., Maravelis, A., Catuneanu, O., Zelilidis, A., 2023. Controls on sedimentation in a deep-water foredeep: Central Pindos foreland basin, western Greece. Basin Research (early view). https://doi.org/10.1111/bre.12804

Bourli, N., Pantopoulos, G., Maravelis, A. G., Zoumpoulis E., Iliopoulos, G., Pomoni-Papaioannou, F., Kostopoulou, S., Zelilidis, A., 2019a. Late Cretaceous to Early Eocene geological history of the eastern Ionian Basin, southwestern Greece: an integrated sedimentological and bed thickness statistics analysis. Cretaceous Research, 98:47–71. https://doi.org/10.1016/j.cretres.2019.01.026

Bourli, N., Kokkaliari, M., Iliopoulos, I., Pe-Piper, G., Piper, D. J. W., Maravelis, A. G., Zelilidis, A., 2019b. Mineralogy of siliceous concretions, Cretaceous of Ionian zone, western Greece: implication for diagenesis and porosity. Marine and Petroleum Geology, 105:45–63. https://doi.org/10.1016/j.marpetgeo.2019.04.011

Cundy, A. B., Gaki-Papanastassiou, K., Papanastassiou, D.,

Maroukian, H., Frogley, M. R., Cane, T. 2010. Geological and geomorphological evidence of recent coastal uplift along a major Hellenic normal fault system (the Kamena Vourla fault zone, NW Evoikos Gulf, Greece). Marine Geology, 271(1-2), 156-164. https://doi.org/10.1016/j.margeo.2010.02.009

D'Angeli, I.M., Vattano, M., Parise, M., De Waele, J., 2017. The Coastal Sulfuric Acid Cave System of Santa Cesarea Terme (Southern Italy). In: Klimchouk, A., N. Palmer, A., De Waele, J., Auler, A. S., Audra, P. (eds) Hypogene Karst Regions and Caves of the World. Cave and Karst Systems of the World, pp. 161-168, Springer, Cham. https://doi.org/10.1007/978-3-319-53348-3_9

D'Angeli, I. M., Parise, M., Vattano, M., Madonia, G., Galdenzi, S., De Waele, J., 2019. Sulfuric acid caves of Italy: A review. Geomorphology, 333, 105-122. https://doi.org/10.1016/j.geomorph.2019.02.025

De Graciansky P.C., De Dardeau G., Lemoine M., Tricart P., 1989. The inverted margin of the French Alps. Journal of the Geological Society of London, Special publ 44(1):87–104. https://doi.org/10.1144/GSL.SP.1989.044.01.06

De Waele, J., Audra, P., Madonia, G., Vattano, M., Plan, L., D'angeli, I. M., Bigot, J.-Y. Nobécourt, J.-C., 2016. Sulfuric acid speleogenesis (SAS) close to the water table: examples from southern France, Austria, and Sicily. Geomorphology, 253, 452-467. https://doi.org/10.1016/j.geomorph.2015.10.019

De Waele, J., D'Angeli, I.M., Audra, P., Plan, L., Palmer, A.N., 2024. Sulfuric acid caves of the world: A review. Earth-Science Reviews, 250, 104693. https://doi.org/10.1016/j.earscirev.2024.104693

Doutsos, T., Piper, G., Boronkay, K., Koukouvelas, I., 1993. Kinematics of the Central Hellenides. Tectonics 12:936–953. https://doi.org/10.1029/93TC00108

Dublyansky, Y. V., 2013. 6.6 Karstification by Geothermal Waters. In: Schroder, J. & Frumkin, A. (eds.) Treatise on Geomorphology, pp. 57–71. San Diego, CA. http://dx.doi.org/10.1016/B978-0-12-374739-6.00110-X

Etiope, G., Papatheodorou, G., Christodoulou, D.P., Ferentinos, G., Sokos, E., Favali, P., 2006. Methane and hydrogen sulfide seepage in the northwest Peloponnesus petroliferous basin (Greece): origin and geohazard. AAPG Bulletin, 90(5):701–713. https://doi.org/10.1306/11170505089

Fernandez-Martinez, A., Román-Ross, G., Cuello, G. J., Turrillas, X., Charlet, L., Johnson, M. R., Bardelli, F., 2006. Arsenic uptake by gypsum and calcite: Modelling and probing by neutron and X-ray scattering. Physica B: Condensed Matter, 385, 935-937.

Farrant, A. R., Smart, P. L., 2011. Role of sediment in speleogenesis; sedimentation and paragenesis. Geomorphology, 134(1-2), 79-93. https://doi.org/10.1016/j.geomorph.2011.06.006

Ganas, A., White, K., Wadge, G., 1997. SPOT DEM analysis for fault segment mapping in the Lokris region, central Greece. EARSEL advances in remote sensing, 5, 46-53.

Hill, C., 1995. Sulfur redox reactions: Hydrocarbons, native sulfur, Mississippi Valley-type deposits, and sulfuric acid karst in the Delaware Basin, New Mexico and Texas. Environmental Geology 25, 16–23. https://doi.org/10.1007/BF01061826

Jones, D. S., Polerecky, L., Galdenzi, S., Dempsey, B. A., Macalady, J. L., 2015. Fate of sulfide in the Frasassi cave system and implications for sulfuric acid speleogenesis. Chemical Geology, 410, 21-27. https://doi.org/10.1016/j.chemgeo.2015.06.002

Karakitsios, V., 1995. The influence of preexisting structure and halokinesis on organic matter preservation and thrust system evolution in the Ionian basin, northwestern Greece: AAPG Bulletin, 79: 960–980. https://doi.org/10.1306/8D2B2191-171E-11D7-8645000102C1865D

Karakitsios, V., 2013. Western Greece and Ionian Sea petroleum systems. AAPG Bulletin, 97 (9): 1567–1595. https://doi.org/10.1306/02221312113

Kesler, E.S., 2005. Fluids in Planetary Systems: ore-Forming Fluids. Elements, 1(1): 13–18.

Klimchouk, A., 2017. Types and Settings of Hypogene Karst. In: Klimchouk, A., N. Palmer, A., De Waele, J., Auler, A.S., Audra, P. (eds) Hypogene Karst Regions and Caves of the World. Cave and Karst Systems of the World, pp. 1-39. Springer, Cham. https://doi.org/10.1007/978-3-319-53348-3_1

Klimchouk, A. B., Eftimi, R., Andreychouk, V. N., 2022. Hypogene karst in the External Albanides and its pronounced geomorphological effect. Proceedings of the 18th International Congress of Speleology, Vol. IV - Karstologia Mémoires n°24, Geomorphology and Speleogenesis: 205-208, Savoie Mont-Blanc.

Lazaridis, G., 2017. Hypogene Speleogenesis in Greece. In: Klimchouk, A., N. Palmer, A., De Waele, J., Auler, A. S., Audra, P. (eds) Hypogene Karst Regions and Caves of the World. Cave and Karst Systems of the World, pp. 225-239, Springer, Cham. https://doi.org/10.1007/978-3-319-53348-3_14

Lazaridis, G., Melfos, V., Papadopoulou, L., 2011. The first cave occurrence of orpiment (As_2S_3) from the sulfuric acid caves of Aghia Paraskevi (Kassandra Peninsula, N. Greece). International Journal of Speleology, 40: 133-139. http://dx.doi.org/10.5038/1827-806X.40.2.6

Manakos, A., 1999. Hydrogeological behavior and sto-

chastic simulation of Krania Elassona karstic aquifer, Thessaly. [PhD Thesis] Aristotle University of Thessaloniki, pp. 214.

Manakos, A., Ntona, M. M., Kazakis, N., Chalikakis, K., 2018. Enhanced characterization of the Krania–Elassona structure and functioning allogenic karst aquifer in central Greece. Geosciences, 9(1): 15. https://doi.org/10.3390/geosciences9010015

Maravelis, A.G., Makrodimitras, G., Zelilidis, A., 2012. Hydrocarbon prospectivity in western Greece. Oil and gas European Magazine 38(2): 84-89.

Merdenisianos, K., 1994. Thermal caves "Kaiafa" and "Kounoupeli" of the Prefecture of Ilia: thermal cave of "Anigridon Nymphon" of Kaiafa baths of the prefecture of Ilia. Bulletin of the Hellenic Speleological Society, 21, pp. 413-426.

Onac, B. P., Sumrall, J.G., Tamas, T., Povara, I., Kearns, J., Darmiceanu, V., Veres, D.S., Lascu, C., 2009. The relationship between cave minerals and H_2S-rich thermal waters along the Cerna Valley (SW Romania). Acta Carsologica, 38(1): 67-79.

Onac, B. P., Forti, P., 2011. State of the art and challenges in cave minerals studies. Studia UBB Geologia, 56(1): 33-42. http://dx.doi.org/10.5038/1937-8602.56.1.4

Onac, B. P., Wynn, J. G. Sumrall, J. B., 2011. Tracing the sources of cave sulfates: a unique case from Cerna Valley, Romania. Chemical Geology, 288, 105-114. https://doi.org/10.1016/j.chemgeo.2011.07.006

Ottens, B., Voudouris, P., 2018. Griechenland: Mineralien-Fundorte-Lagerstätten, Christian Weise Verlag, Munchen, Germany, 480 pp. ISBN 978-3-921656-86-0.

Pe-Piper, G., Doutsos, T., Mijara, A., 1993. Petrology and regional significance of the Hercynian granitoid rocks of the Olympiada area, northern Thessaly, Greece. Chemie der Erde Geochemistry 53, 21–36.

Petrocheilou, A., 1974. The cave "Peristeri" in Megalochori, Methana. Bulletin of Hellenic Speleological Society, 12(5): 142-151.

Plan, L., Tschegg, C., De Waele, J., Spötl, C., 2012. Corrosion morphology and cave wall alteration in an Alpine sulfuric acid cave (Kraushöhle, Austria). Geomorphology, 169, 45-54. https://doi.org/10.1016/j.geomorph.2012.04.006

Polyak, V. J., Provencio, P., 2001. By-product materials related to H_2S-H_2SO_4 influenced speleogenesis of Carlsbad, Lechuguilla, and other caves of the Guadalupe Mountains, New Mexico. Journal of Cave and Karst Studies, 63(1): 23-32.

Rieck, B., Kolitsch, U., Voudouris, P., Giester, G., Tzeferis, P., 2018. More new finds from Lavrion, Greece. Mineralien Welt 5, 32-77 (in German).

Swezey, C.S., Piatak, N.M., Seal, R.R., Wandless G.A., 2002. Sulfur and oxygen isotopic composition of gypsum in caves of Virginia and West Virginia. Geological Society of America, Abstracts with Programs, 34: 231.

Temovski, M., Audra, P., Mihevc, A., Spangenberg, J. E., Polyak, V., McIntosh, W., Bigot, J. Y., 2013. Hypogenic origin of Provalata Cave, Republic of Macedonia: a distinct case of successive thermal carbonic and sulfuric acid speleogenesis. International Journal of Speleology, 42(3), 7. http://dx.doi.org/10.5038/1827-806X.42.3.7

Temovski, M., Futó, I., Túri, M., Palcsu, L., 2018. Sulfur and oxygen isotopes in the gypsum deposits of the Provalata sulfuric acid cave (Macedonia). Geomorphology, 315, 80-90. https://doi.org/10.1016/j.geomorph.2018.05.010

Vasileiou, E., Koumantakis, I., 2013. The role of Kefalovruso and Amourio springs in the hydrodynamic conditions of Potamia Elassona Basin. Bulletin of the Geological Society of Greece, 47(2), 801-810.

Vaxevanopoulos, M., 2006. Tectonic conditions in the speleogenetic process of Melissotripa cave in Kefalovriso of Elassona (Central Greece) [Msc Thesis]. Aristotle University of Thessaloniki, 1-106 pp.

Vourlakos, N.M., Fitros, M.G., 2019. The Minerals of Lavrion; The Scientific Society of Lavreotiki: Lavrion, Greece, No. 13; ISBN 978-960-85333-6.

Webb, J. A., 2021. Supergene sulphuric acid speleogenesis and the origin of hypogene caves: evidence from the Northern Pennines, UK. Earth Surface Processes and Landforms, 46(2): 455-464. https://doi.org/10.1002/esp.5037

White, W. B., 2015. Minerals and speleothems in Burnsville Cove caves. The Caves of Burnsville Cove, Virginia: Fifty Years of Exploration and Science, pp. 421-441.

Wynn, J. G., Sumrall, J. B., Onac, B. P., 2010. Sulfur isotopic composition and the source of dissolved sulfur species in thermo-mineral springs of the Cerna Valley, Romania. Chemical Geology, 271, 31-43. https://doi.org/10.1016/j.chemgeo.2009.12.009

Zelilidis, A., Maravelis A.G., Tserolas, P., Konstantopoulos, P.A., 2015. An overview of the Petroleum systems in the Ionian zone, onshore NW Greece and Albania. Journal of Petroleum Geology, 38(3): 331-347. https://doi.org/10.1111/jpg.12614

Zoumpouli, E., Maravelis, A.G., Iliopoulos, G., Botziolis, C., Zygouri, V., Zelilidis, A., 2022. Re-Evaluation of the Ionian Basin Evolution during the Late Cretaceous to Eocene (Aetoloakarnania Area, western Greece). Geosciences; 12(3):106. https://doi.org/10.3390/geosciences12030106.